

# Understanding Reactivity and Stereoselectivity in Palladium-Catalyzed Diastereoselective $sp^3$ C–H Bond Activation: Intermediate Characterization and Computational Studies

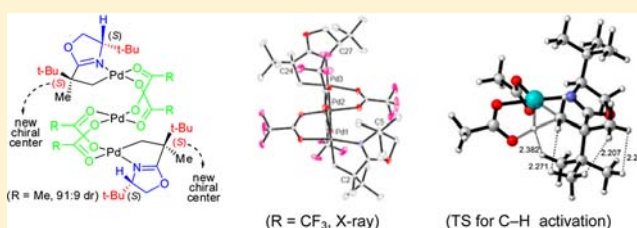
Ramesh Giri,<sup>†</sup> Yu Lan,<sup>‡</sup> Peng Liu,<sup>‡</sup> K. N. Houk,<sup>\*,‡</sup> and Jin-Quan Yu<sup>\*,†</sup>

<sup>†</sup>Department of Chemistry, The Scripps Research Institute, 10550 North Torrey Pines Road, La Jolla, California 92037, United States

<sup>‡</sup>Department of Chemistry and Biochemistry, University of California, Los Angeles, Los Angeles, California 90095, United States

## S Supporting Information

**ABSTRACT:** The origin of the high levels of reactivity and diastereoselectivity (>99:1 dr) observed in the oxazoline-directed, Pd(II)-catalyzed  $sp^3$  C–H bond iodination and acetoxylation reactions as reported in previous publications has been studied and explained on the basis of experimental and computational investigations. The characterization of a trinuclear chiral C–H insertion intermediate by X-ray paved the way for further investigations into C–H insertion step through the lens of stereochemistry. Computational investigations on reactivities and diastereoselectivities of C–H activation of *t*-Bu- and *i*-Pr-substituted oxazolines provided good agreement with the experimental results. Theoretical predictions with DFT calculations revealed that C–H activation occurs at the monomeric Pd center and that the most preferred transition state for C–H activation contains two sterically bulky *t*-Bu substituents in anti-positions due to steric repulsion and that this transition state leads to the major diastereomer, which is consistent with the structure of the newly characterized C–H insertion intermediate. The structural information about the transition state also suggests that a minimum dihedral angle between C–H bonds and Pd–OAc bonds is crucial for C–H bond cleavage. We have also utilized density functional theory (DFT) to calculate the energies of various potential intermediates and transition states with *t*-Bu- and *i*-Pr-substituted oxazolines and suggested a possible explanation for the substantial difference in reactivity between the *t*-Bu- and *i*-Pr-substituted oxazolines.



## 1. INTRODUCTION

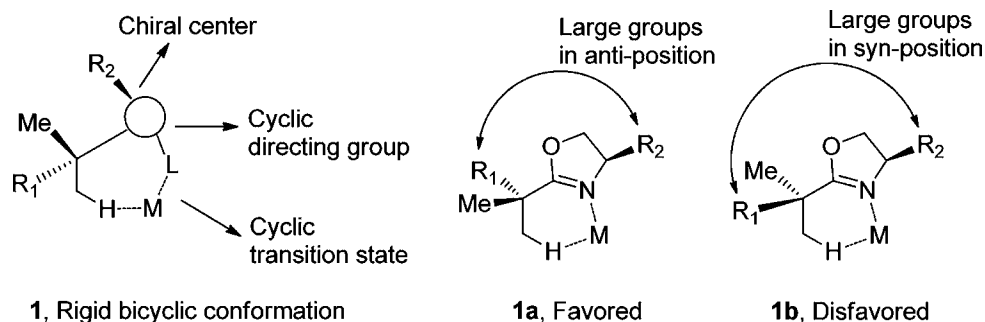
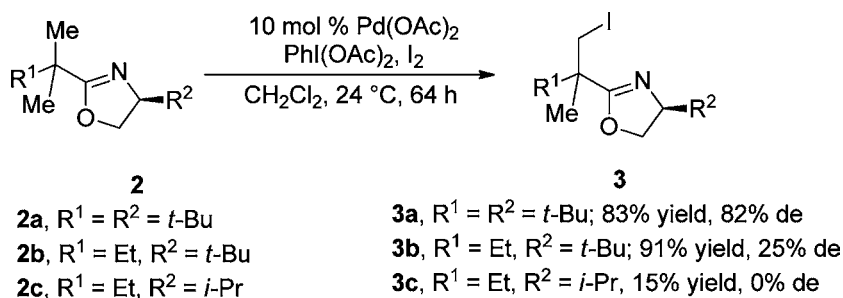
Transition-metal-catalyzed activation/functionalization of unactivated C–H bonds has been the subject of great research interest in recent years.<sup>1,2</sup> Among the plethora of transition-metal-catalyzed processes, palladium-catalyzed reactions, in particular, have enjoyed a prominent standing in the C–H activation field.<sup>3</sup> In addition to innovation of diverse reactions, mechanistic details on the C–H cleavage step<sup>4–8</sup> and redox chemistry for bond formation,<sup>9</sup> are being meticulously investigated experimentally and theoretically. Despite remarkable progress in these two frontiers with palladium catalysts, stereoselective cleavage of unactivated prochiral C–H bonds and its mechanistic aspects have been little explored.<sup>10</sup> The diastereotopic C–H bonds at the carbon atom are selectively cleaved on a metal center under the influence of a proximal chiral center tethered to it via a removable linkage.<sup>11</sup> Tolman and co-workers observed a moderate level of diastereoselectivity in the intramolecular activation of  $sp^3$  C–H bonds in a rhodium dicarbonyl complex of  $C_3$ -symmetric TpMenth ligand.<sup>12</sup> Although these metal-mediated reactions show stereoselectivity during the C–H activation step, subsequent functionalization of the metallacycles has been realized only in limited cases. Sames and co-workers have described the total synthesis of (–)-rhazinilam based on the diastereoselective

dehydrogenation of an ethyl group via C–H activation by attaching a synthetic intermediate to a stoichiometric dialkyl Pt-chiral oxazoline complex through an imine linkage.<sup>13</sup> Tremendous efforts have also been devoted to develop transition-metal-catalyzed asymmetric C–H functionalization in the areas of allylic acetoxylation,<sup>14</sup> biomimetic oxidation,<sup>15</sup> addition of arene to alkene,<sup>16</sup> and carbenoid/nitrenoid insertion.<sup>2,17</sup> In this regard, we reported a rare example of auxiliary-controlled asymmetric Pd insertion into both  $sp^2$  and  $sp^3$  C–H bonds. Selection of an appropriate auxiliary or directing group that would effect C–H bond cleavage with palladium catalysts under mild conditions is crucial for high stereoselectivity. While asymmetric induction through installation of chiral auxiliary is a well-established procedure in organic synthesis,<sup>18</sup> extension of this approach to the catalytic, stereoselective activation of C–H bonds is largely unexplored. We were encouraged by Meyer's  $\alpha$ -lithiation/alkylation chemistry, where chiral oxazolines provide high levels of asymmetric induction,<sup>19</sup> and the success of using chiral oxazolines as ligands in asymmetric catalysis.<sup>20</sup> Furthermore, previously observed oxazoline-directed cyclopalladation reac-

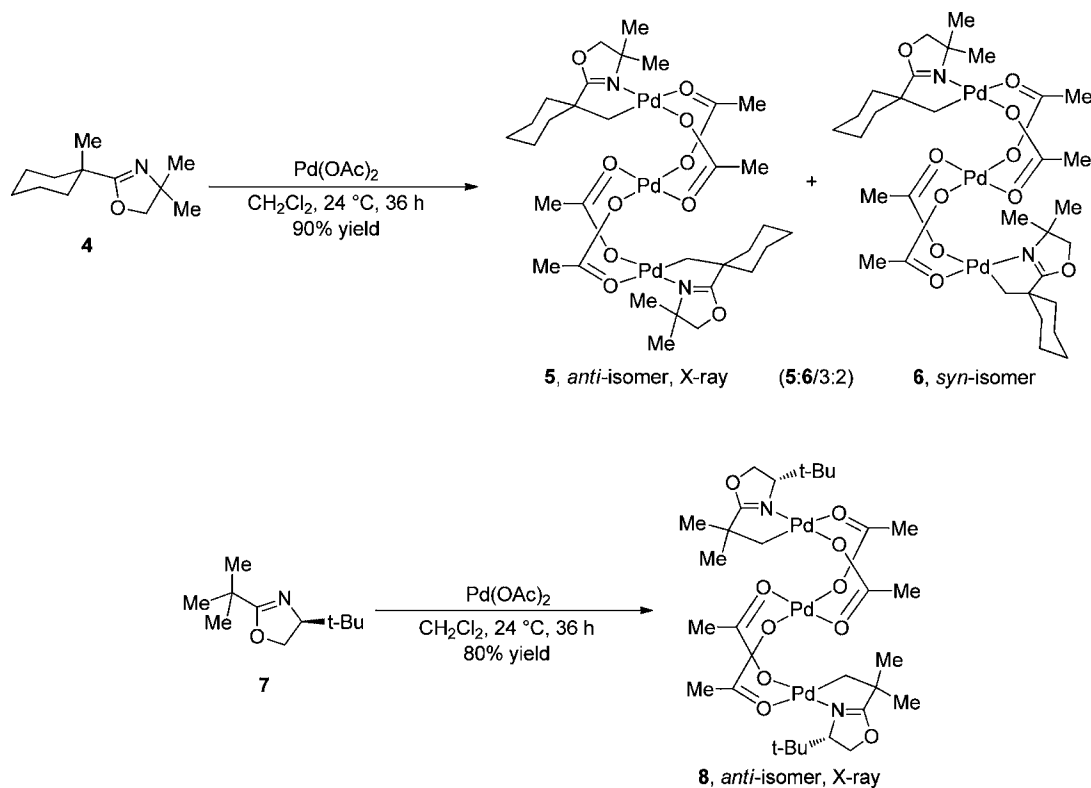
Received: May 18, 2012

Published: July 25, 2012

Scheme 1. Working Model for Diastereoselective C–H Cleavage

Scheme 2. Diastereoselective C–H Iodination with *i*-Pr- and *t*-Bu-Substituted Oxazoline Auxiliaries

Scheme 3. Trinuclear Pd(II) Complexes with Achiral and Chiral Oxazolines

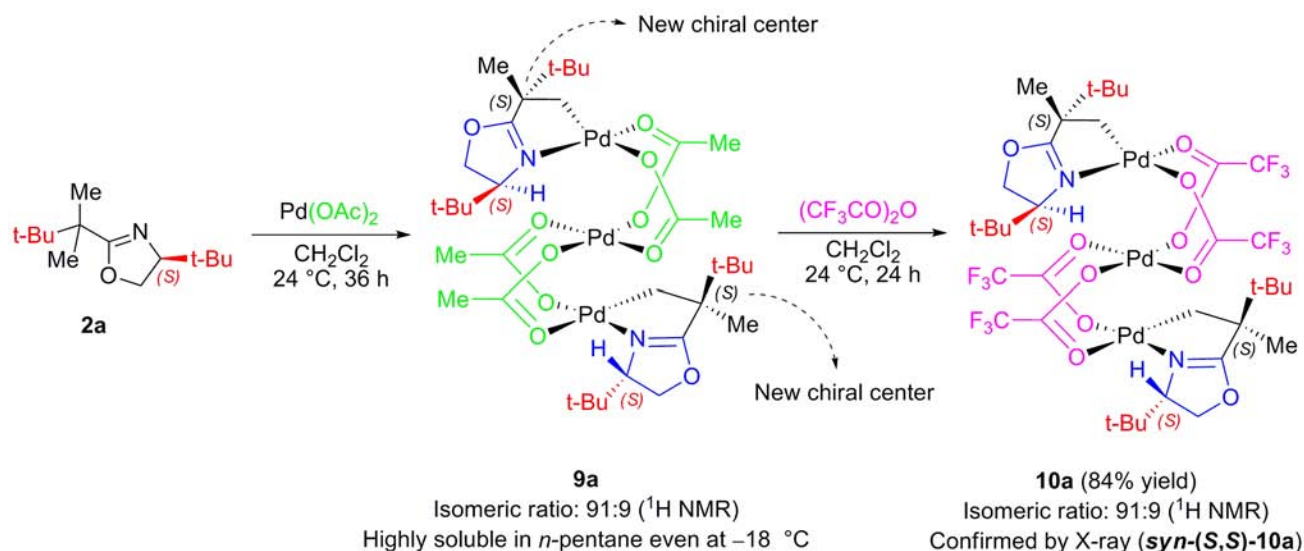


tions of both  $sp^2$  and  $sp^3$  C–H bonds<sup>21</sup> also provided the foundation for our exploratory studies.

We began our investigation by proposing a working steric model for diastereoselective cleavage of C–H bonds on organic molecules pre-coordinated to a transition metal through a removable, nonracemic, chiral linkage (Scheme 1). Since  $\sigma$ -chelation-assisted C–H activation takes place through a cyclic

transition state,<sup>5</sup> we envisioned that the selection of oxazoline as a cyclic chiral auxiliary would provide an efficient stereocontrol by forming a conformationally rigid bicyclic transition state **1** during C–H bond cleavage. As a consequence, the chiral auxiliary could induce high levels of stereoselectivity during C–H activation in conjunction with a bicyclic conformation via a steric repulsion model outlined in

Scheme 4. Determination of the Absolute Stereochemistry of C–H Activation



Scheme 1. Transition state **1a**, in which the sterically bulky  $\text{R}^1$  and  $\text{R}^2$  groups are in anti-position, is favored over **1b** due to reduced steric repulsion between Me and  $\text{R}^2$  when  $\text{R}^1$  is larger than the Me group. Predominant C–H activation pathway through transition state **1a** will give the major stereoisomer. We anticipate that this primitive model requires further elaboration.

Our early investigations in 2002 were long baffled by the lack of reactivity and stereoselectivity of oxazolines bearing a 4-*i*-Pr group such as **2c** ( $\text{R}^1 = \text{Et}$ ,  $\text{R}^2 = i\text{-Pr}$ ; 15% yield, 0% de) for the iodination of  $\beta\text{-C-H}$  bonds (Scheme 2). Strikingly, reactions proceeded with high yields and moderate diastereoselectivity when the 4-*i*-Pr group was replaced by a 4-*t*-Bu group (**2b**,  $\text{R}^1 = \text{Et}$ ,  $\text{R}^2 = t\text{-Bu}$ ; 91% yield, 25% de). Moreover, substitution of an Et group at the  $\alpha$ -position of the parent carboxylic acid with a sterically demanding *t*-Bu group, such as in oxazoline **2a**, afforded monoiodinated product **3a** in 83% yield with a high level of diastereoselectivity (82% de) (Scheme 2).

Intrigued by the dramatic change in reactivity and stereoselectivity with subtle alterations in the steric environment on the oxazoline ring, we have sought, in the present study, to elucidate the mechanism and origin of reactivity and diastereoselectivity through the preparation and characterization of a reactive intermediate formed after diastereoselective C–H activation and through computational studies on the energies of possible intermediates and transition states leading to the isolated intermediate using density functional theory (DFT).<sup>22</sup> Our computational investigation has revealed that the reactions with *i*-Pr- and *t*-Bu-substituted oxazolines involve different catalyst resting states before C–H activation and that the lower reactivity of an *i*-Pr-substituted oxazoline results from greater stability of its catalyst resting state, which accounts for higher overall activation barrier for C–H cleavage. We have also characterized by a single crystal X-ray crystallography the major isomer of a chiral trinuclear palladacycle formed after diastereoselective cleavage of a  $\beta\text{-C-H}$  bond of a chiral oxazoline bearing two diastereotopic methyl groups. In excellent agreement with the solid-state structure, theoretical predictions with DFT calculations also revealed that the most preferred transition state for C–H activation in oxazoline substrates contains sterically bulky substituents at the  $\alpha$ -position of parent carboxylic acid and the oxazoline ring in anti-

positions due to steric repulsion and that this transition state leads to the major diastereomer.

## 2. RESULTS AND DISCUSSION

We previously prepared the cyclopalladated trinuclear complexes **5**, **6**, and **8** of achiral and chiral oxazolines **4** and **7** (Scheme 3).<sup>9,23</sup> These palladacycles are potential intermediates in the Pd(II)-catalyzed iodination and acetoxylation of unactivated C–H bonds.<sup>9</sup> First, these palladacycles maintain trinuclear integrity in the reaction solvent ( $\text{CH}_2\text{Cl}_2$ ). The trinuclear complexes distinguish themselves from dimer and monomer by the ratio of acetate groups to oxazoline units, as indicated by  $^1\text{H NMR}$ . Second, they react with iodine and peroxide/acetic anhydride at room temperature to afford the iodinated and acetoxylation products in high yields. Examination of the X-ray crystal structures of the highly reactive trinuclear Pd(II) complexes **5** and **8** led us to propose a stereomodel to account for diastereoselectivity.<sup>24</sup> In sharp contrast to the 3:2 mixture of anti- and syn-complexes **5** and **6** formed from achiral oxazoline **4**, only the anti-isomer **8** was obtained from the chiral oxazoline **7**. However, we had not characterized intermediates that contain chiral centers on both auxiliary and substrate, which are crucial for elucidating the stereomodel and transition state.

To gain insights into the absolute stereochemistry of the observed C–H activation, we prepared the cyclometalated intermediate **9a** from the reaction of  $\text{Pd}(\text{OAc})_2$  with the chiral oxazoline **2a** containing diastereotopic methyl groups on the parent carboxylic acid moiety (Scheme 4). The complex **9a** contains a mixture of isomers in a 91:9 ratio, which approximately corresponds to the observed diastereoselectivity. The complex **9a** is highly soluble in *n*-pentane even at  $-18^\circ\text{C}$ , and its purification and crystallization proved extremely difficult. However, we discovered that the bridging  $\mu$ -acetate groups could be easily exchanged with  $\mu$ -trifluoroacetate groups without losing the stereoisomeric ratio (91:9) by simply stirring the complex **9a** in trifluoroacetic anhydride for 24 h at room temperature. We were then able to isolate palladacycle **10a** with bridging  $\mu$ -trifluoroacetate groups and grow a single crystal at  $-18^\circ\text{C}$ , which was characterized to be the major isomer *syn*-(*S,S*)-**10a** by X-ray crystallography (Figure 1). As predicted, the



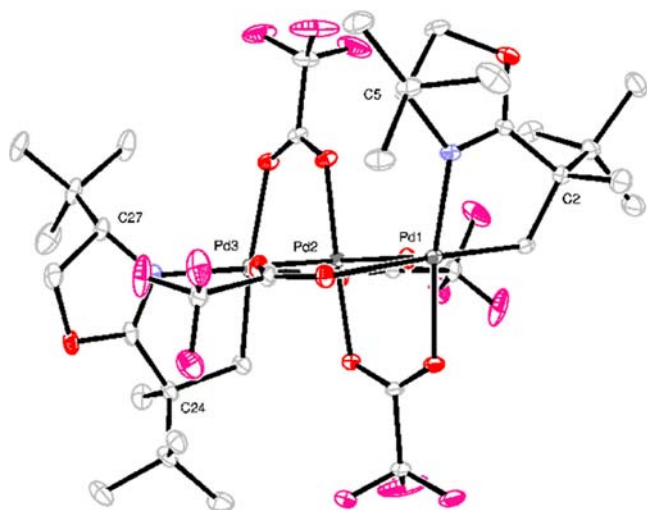


**Figure 1.** ORTEP diagram of palladacycle *syn*-(*S,S*)-**10a**. Selected bond lengths (Å) and angles (deg): C1–Pd1, 1.991(8); C23–Pd3, 1.994(8); N1–Pd1, 2.001(6); N2–Pd3, 2.023(6); Pd1–Pd2, 2.9458(8); Pd2–Pd3, 2.9539(8); C1–Pd1–N1, 81.0(3); C23–Pd3–N2, 83.1(3).

*t*-Bu groups on the carboxylic acid and oxazoline moieties were oriented in anti-positions at both termini of the trinuclear palladacycle *syn*-(*S,S*)-**10a**. As a result, the newly generated chiral center assumed (*S*)-configuration.<sup>25</sup> Moreover, the reaction of  $\mu$ -acetato palladacycle **9a** with iodine affords the iodinated product in the same diastereoisomeric ratio (91:9).

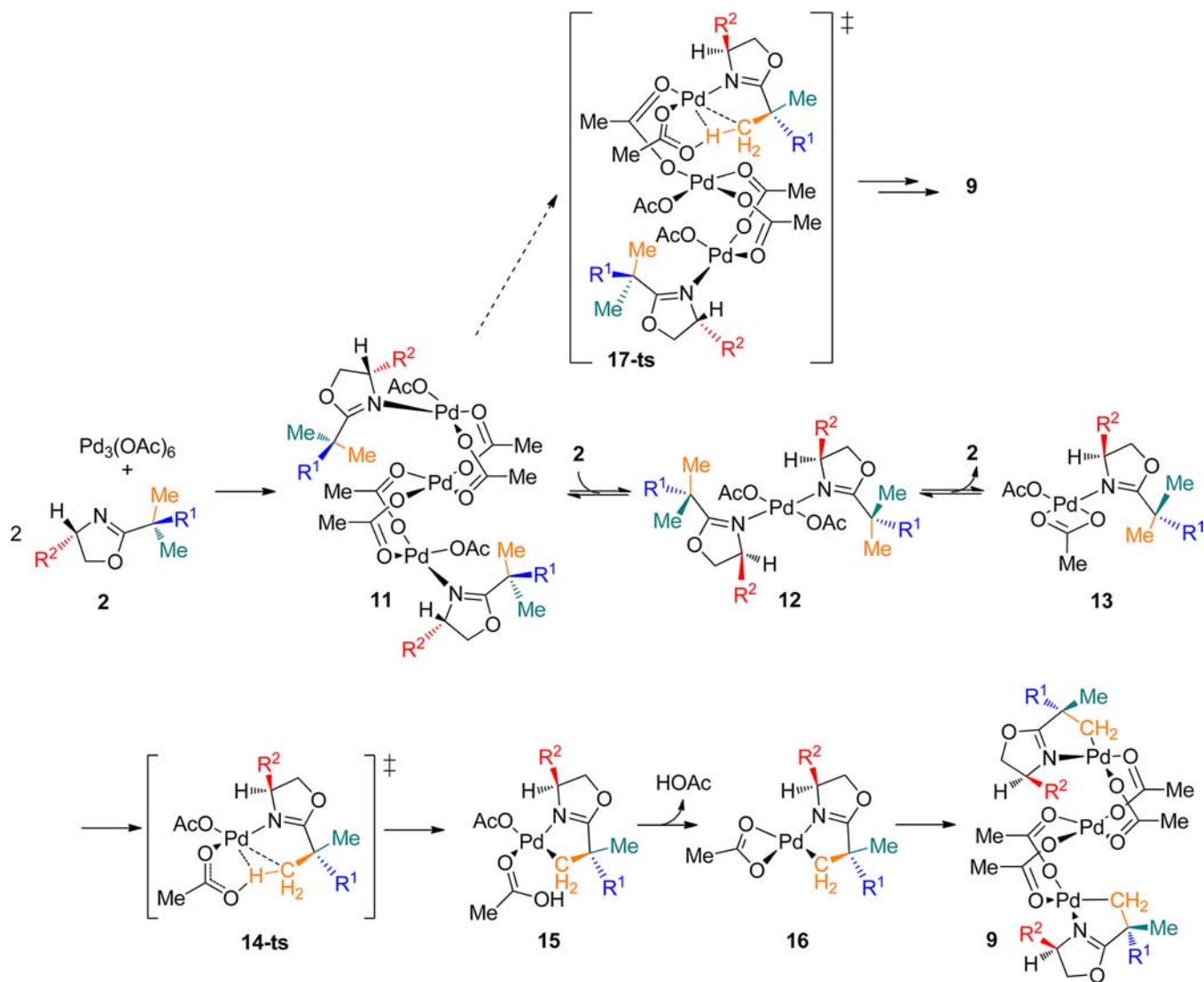
To further investigate the effects of substituents on reactivity and the origin of the high level of diastereoselectivity during the C–H bond cleavage, we performed DFT studies to calculate the energies of different intermediates and transition states leading to the formation of trinuclear intermediate **9**. Despite extensive computational studies on C–H cleavage involving  $\text{ArPdX}(\text{PPh}_3)$  species by Maseras and Echavarren,<sup>4</sup> and Fagnou,<sup>6</sup> the understanding of cyclopalladation reactions with Pd(II) catalysts remains less developed. In an early mechanistic study of aryl C–H cyclopalladation, Martinez proposed a proton abstraction pathway involving a four-membered transition state.<sup>26</sup> Subsequent computational work by Davies and Macgregor in 2005 supported a similar mechanism, but involving a six-membered transition state.<sup>5</sup> These computational studies indicated that a vacant coordination site on palladium is necessary for insertion into the C–H bond. On the basis of these previous mechanistic studies, a proposed mechanism of the formation of trinuclear palladacycle **9** is outlined in Scheme 5. The  $\text{Pd}_3(\text{OAc})_6$  trimer<sup>27</sup> reacts with two molecules of oxazoline **2** to generate intermediate **11**, which dissociates upon further coordination with **2** to form monomeric intermediates **12** or **13** with either two or one oxazolines bound to Pd. The Pd in **12** and **13** adopts a square planar geometry. In intermediate **13**, one of the acetato groups is  $\eta$ -2-coordinated to palladium while the other acetato is  $\eta$ -1-coordinated. The  $\eta$ -2 acetato isomerizes to be  $\eta$ -1-coordinated and releases a vacant coordination site on Pd for subsequent C–H activation. In the C–H activation transition state **14-ts**, the cleavage of the C–H bond and formations of the Pd–C and AcO–H bonds are concerted. The structure of **14-ts** suggests that maintaining a minimum dihedral angle between C–H bonds and Pd–OAc bonds is essential for high reactivity. The C–H activation leads to a monomeric palladacycle

intermediate **15**. After the release of acetic acid, the trimeric palladacycle complex **9** is generated. Alternatively, the C–H activation may occur with the Pd trimer **11** via transition state **17-ts** instead of its dissociation to monomeric Pd species before C–H activation. This requires breaking one of the bridged acetato groups to generate a free coordination site on Pd for C–H activation. Both pathways were considered in the computational investigations.

The free energy profiles of C–H activation of oxazolines **2a** ( $\text{R}^1 = t\text{-Bu}$ ,  $\text{R}^2 = t\text{-Bu}$ ) and **2c** ( $\text{R}^1 = \text{Et}$ ,  $\text{R}^2 = i\text{-Pr}$ ) are shown in Figure 2. Coordination of two molecules of oxazoline **2c** to the  $\text{Pd}_3(\text{OAc})_6$  trimer to form complex **11c** is exergonic by 6.8 kcal/mol. The same process with bulkier oxazoline **2a** to form **11a** is endergonic by 9.3 kcal/mol. Further coordination of oxazoline **2c** leads to decomposition of complex **11c** to form monomeric [bis(oxazoline)]Pd(OAc)<sub>2</sub> complex **12c**, which is 10.4 kcal/mol more stable than  $\text{Pd}_3(\text{OAc})_6$ . In the reaction with oxazoline **2a**, the Pd monomer complex **12a** is 2.5 kcal/mol less stable than  $\text{Pd}_3(\text{OAc})_6$ . Dissociation of one molecular oxazoline from **12a** and **12c** to form **13a** and **13c** is endergonic by 6.9 and 17.1 kcal/mol, respectively. Thus, in the reaction with the bulkier oxazoline **2a**, the catalyst resting state before C–H activation is  $\text{Pd}_3(\text{OAc})_6$ , while in the reaction with **2c**, the resting state is the monomeric [bis(oxazoline)]Pd(OAc)<sub>2</sub> complex **12c**. The stability of the resting state **12c** leads to significantly higher overall activation energies for C–H activation of oxazoline **2c**. Although the C–H activation transition state **14c-ts** is only 1.8 kcal/mol less stable than **14a-ts**, the overall activation barrier for reaction with **2c** is 38.4 kcal/mol (**12c**  $\rightarrow$  **14c-ts**), much higher than that for the reaction with **2a** in which the overall barrier is 26.2 kcal/mol [ $\text{Pd}_3(\text{OAc})_6 \rightarrow$  **14a-ts**]. The C–H activation leads to the five-membered metallacycle intermediate, **15a**, and **15c**, respectively. Subsequent elimination of acetic acid from **15a** and **15c** leads to **16a** and **16c**; both are a few kcal/mol less stable than **15a/c** in terms of Gibbs free energies. Association of two molecules of **16a/c** and Pd(OAc)<sub>2</sub> forms stable trinuclear Pd metallacycles **9a** and **9c**. Both **9a** and **9c** are  $\sim$ 11 kcal/mol more stable than the monomeric metallacycle **15a** and **15c**. We have also computed single point solvation energy corrections using the SMD model, and the results are summarized in the Supporting Information. In the solvation-corrected free energy diagram, the maximum deviations from the gas-phase results are within a few kcal/mol. The relative activation free energies in the gas phase and in solution only differ by a few tenths of a kcal/mol. These solvation effects do not change any conclusions of the gas-phase results.

The alternative pathway that involves C–H activation directly from the trinuclear complexes **11a** and **11c** is less favorable than the mononuclear pathway described above. Trinuclear C–H activation transition states **17a-ts** and **17c-ts** are 7.2 and 3.1 kcal/mol less favorable than the corresponding mononuclear C–H activation transition states (**14a-ts** and **14c-ts**, respectively). The C–H activation from the trinuclear complex requires breaking one of the bridged acetato groups to generate a free coordination site on Pd. This leads to the higher activation energies of the trinuclear pathway.

The optimized geometries of the bis(oxazoline) Pd complexes **12a** and **12c** are shown in Figure 3. Complex **12a** is destabilized due to steric repulsions of the *t*-Bu ( $\text{R}^2$ ) groups with the acetate. In **12a**, the shortest O–H distances between the *t*-Bu hydrogen and acetate oxygen atoms are 2.21 and 2.43

Scheme 5. Proposed Mechanism of the Pd(OAc)<sub>2</sub> Catalyzed C–H Activation of Oxazoline 2

Å. By replacing the *t*-Bu group with an *i*-Pr group, the complex 12c is much less crowded and thus more stable than 12a.

We then investigated the origin of stereoselectivity in C–H activations of oxazolines 2a–c. For each oxazoline, the C–H activation may occur via four possible transition states (14-ts1–14-ts4, Scheme 6). The optimized geometries of the C–H activation transition states with oxazoline 2a are shown in Figure 4. All four transition states involve simultaneous cleavage of the C–H bond and formation of the AcO–H and Pd–C bonds as well as strong Pd–H interaction, which indicate a concerted metalation–deprotonation mechanism and a rigid cyclic transition state structure. The six-membered cycle that involves Pd, two atoms in the oxazoline ring, the prochiral  $\alpha$ -carbon, and the C–H bond being cleaved adopts a half-chair conformation. In 14-ts1 and 14-ts3, the proton being transferred is above the Pd–oxazoline plane, and the  $\alpha$ -substituent that is syn to R<sup>2</sup> (Me and R<sup>1</sup> in 14-ts1 and 14-ts3, respectively) is at the axial position. In 14-ts2 and 14-ts4, the syn  $\alpha$ -substituent is equatorial (Me and R<sup>1</sup> in 14-ts2 and 14-ts4, respectively). The R<sup>1</sup> and R<sup>2</sup> groups are anti to each other

in 14-ts1 and 14-ts2, which led to the major diastereomeric (*S,S*)-product. R<sup>1</sup> and R<sup>2</sup> are syn in 14-ts3 and 14-ts4, leading to the minor (*S,R*)-diastereomer. The computed relative activation energies are summarized in Table 1. In the reactions with 2a and 2b, 14-ts1 and 14-ts3 are more than 2 kcal/mol less stable than 14-ts2 and 14-ts4. Transition states 14-ts1 and 14-ts3 are destabilized by steric repulsions between the axial substituents on the  $\alpha$ -carbon and the *t*-Bu (R<sup>2</sup>) on the oxazoline. When a smaller R<sup>2</sup> group (*i*-Pr) is employed, 14-ts1 and 14-ts3 are only a few tenths kcal/mol less stable than 14-ts2 and 14-ts4. In the reactions with all three oxazolines, the diastereoselectivity of the C–H activation product is determined by the energy difference between 14-ts2 and 14-ts4. In the reaction with 2a, 14a-ts2 is 2.3 kcal/mol more stable than 14a-ts4. This suggests the diastereomeric product (*S,S*)-15a is favored with 96% de. In the reactions with 2b and 2c, the energy difference between 14-ts2 and 14-ts4 is diminished, in agreement with the low de observed in experiment.

The energy difference between 14a-ts2 and 14a-ts4 is attributed to the *gauche-t*-Bu/H repulsions around the prochiral

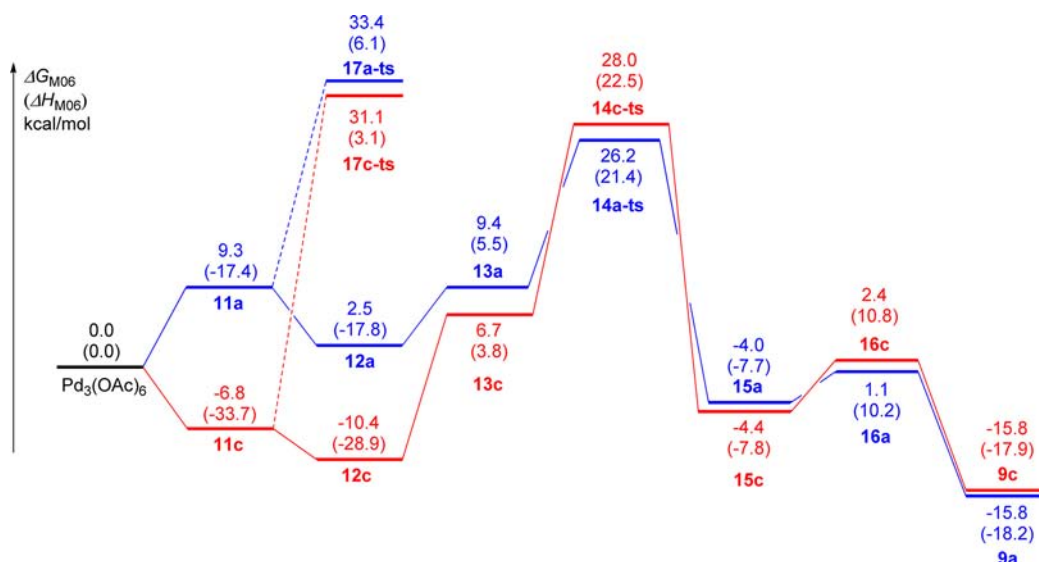


Figure 2. The M06 free energy profile of C–H activation of oxazolines 2a (blue) and 2c (red). Enthalpies are given in parentheses.

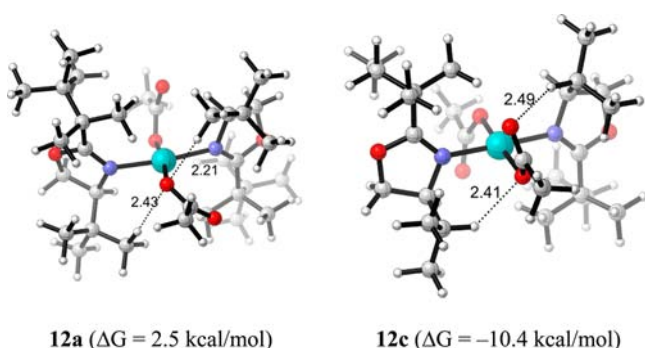


Figure 3. Optimized geometries of [bis(oxazoline)]Pd(OAc)<sub>2</sub> complexes 12a and 12c. Energies are with respect to Pd<sub>3</sub>(OAc)<sub>6</sub>.

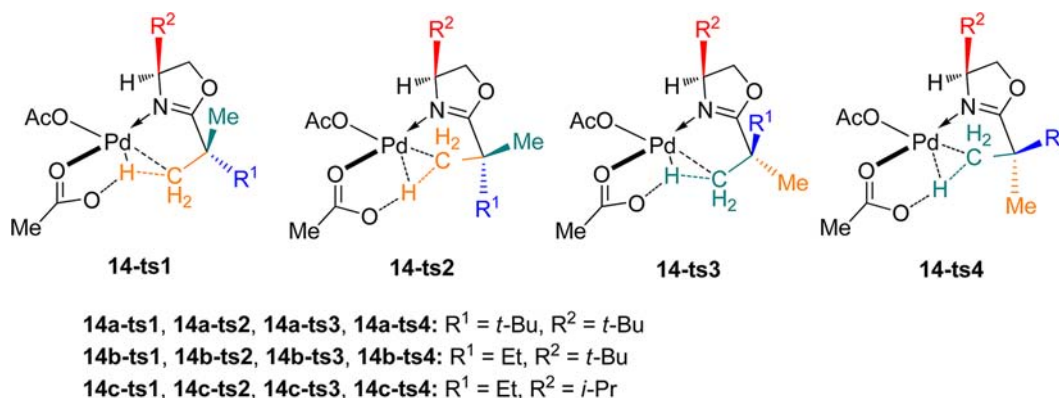
carbon–methyl bond (highlighted in green in Figure 4). The cleaving C–H bond is gauche to the adjacent *t*-Bu group in 14a-ts2 and anti to the *t*-Bu in 14a-ts4 (see the Newman projections in Figure 4). Because the C–H distances in the cleaving C–H bond ( $\sim 1.4$  Å) are significantly longer than a regular C–H bond ( $\sim 1.1$  Å), the *gauche-t*-Bu/H repulsion with the cleaving C–H bond is smaller. In 14a-ts2, there is one regular *gauche-t*-Bu/H interaction with an H–H distance of 2.27 Å between *t*-Bu and H<sub>c</sub>. The *gauche* repulsion with the

cleaving C–H' bond is much weaker, with a significantly longer H–H distance of 2.38 Å between *t*-Bu and H'. In contrast, there are two hydrogens gauche to the *t*-Bu in 14a-ts4, with H–H distances being 2.14 and 2.22 Å, respectively. Thus, 14a-ts4 is less stable than 14a-ts2 due to unfavorable *gauche-t*-Bu/H repulsions. Replacing the *t*-Bu (R<sup>1</sup>) group with the smaller Et, the energy differences between transition states 14b-ts2 and 14b-ts4 and between 14c-ts2 and 14c-ts4 reduced to essentially zero, in agreement with experiment. The *gauche* repulsions between Et and H are much smaller than the *t*-Bu/H repulsions. The Et substitution on R<sup>1</sup> is not sufficient to differentiate the activation of anti and *gauche* C–H bonds, as illustrated in the Newman projections in Figure 4.

### 3. CONCLUSIONS

We have prepared and characterized the major diastereomer of a chiral trinuclear palladacycle that exists as a potential intermediate in the oxazoline-directed, Pd(II)-catalyzed iodination and acetoxylation of sp<sup>3</sup> C–H bonds. Reaction of the chiral trinuclear palladacycle with I<sub>2</sub> provided the iodinated product in the same diastereomeric ratio as that of the catalytic reaction (dr, 91:9). The solid-state structure of the major diastereomer *syn*-(*S,S*)-10a revealed that the two bulky *t*-Bu groups on the oxazoline and carboxylic moieties of the substrate remain in

### Scheme 6. Possible Transition States of the C–H Activation





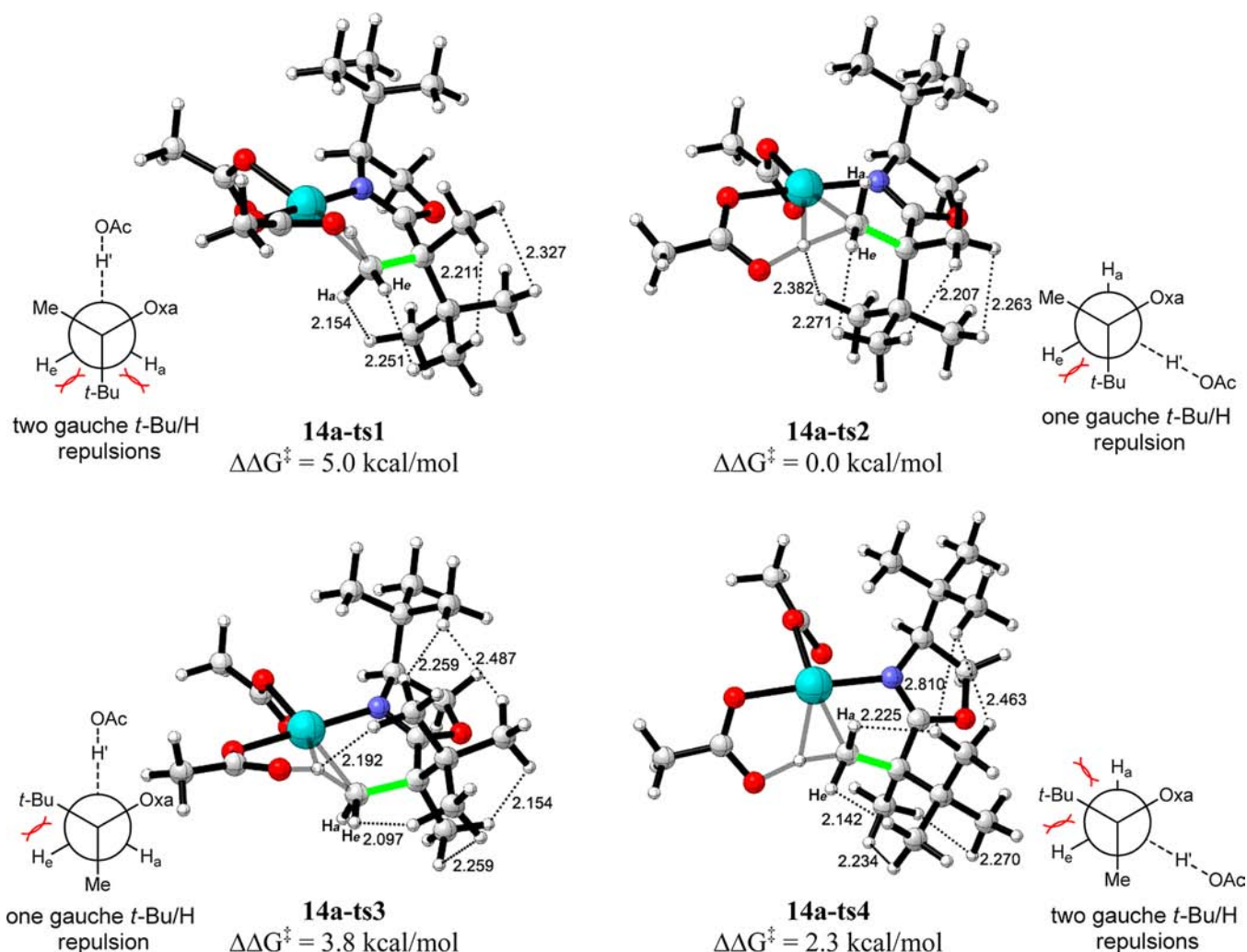


**Figure 4.** Optimized geometries of transition states 14a-ts1, 14a-ts2, 14a-ts3, and 14a-ts4 and the Newman projections about the C–C bond highlighted in green.

**Table 1.** Relative Activation Free Energies and Enthalpies (in parentheses) for the C–H Activation Transition States<sup>a</sup>

oxazoline	R <sup>1</sup>	R <sup>2</sup>	14-ts1	14-ts2	14-ts3	14-ts4	de, %	
							calcd	expl
2a	<i>t</i> -Bu	<i>t</i> -Bu	5.0 (4.7)	0.0 (0.0)	3.8 (3.4)	2.3 (2.2)	96 (96)	82
2b	Et	<i>t</i> -Bu	2.8 (3.0)	0.0 (0.0)	3.6 (3.0)	0.1 (0.2)	8 (17)	25
2c	Et	<i>i</i> -Pr	0.3 (0.6)	0.0 (0.0)	0.8 (0.5)	−0.2 (−0.1)	17 (8)	0

<sup>a</sup>All energies are with respect to 14-ts2 in kcal/mol.

anti-positions to each other and that the new chiral center generated after the C–H cleavage assumed (*S*)-stereochemistry. Computational investigations on reactivities and diastereoselectivities of C–H activation of oxazolines 2a–c provided good agreement with the experimental results. C–H activation most likely occurs at the monomeric Pd center. The most preferred transition state, in which the bulky *t*-Bu substituents on the prochiral carbon (R<sup>1</sup>) and on the oxazoline (R<sup>2</sup>) prefer to be anti to each other, leads to the major diastereomer product *syn*-(*S,S*)-10a. *t*-Bu substitution at the R<sup>2</sup> position is essential to achieve high reactivity. Replacing the R<sup>2</sup> group with the smaller *i*-Pr group leads to formation of a stable resting [bis(oxazoline)]Pd(OAc)<sub>2</sub> complex before the C–H activation and increases the overall activation barrier. In the reaction with *t*-Bu-substituted oxazoline 2a, such a [bis-

(oxazoline)]Pd(OAc)<sub>2</sub> complex is destabilized to form the reactive monomeric intermediate (oxazoline)Pd(OAc)<sub>2</sub> due to steric repulsions with the *t*-Bu groups.

## 4. EXPERIMENTAL SECTION

**4.1. Preparation of Trinuclear Bis- $\mu$ -acetato and Bis- $\mu$ -trifluoroacetato Pd(II) Complexes 9a and 10a.** Oxazoline 2a (113 mg, 0.5 mmol) was stirred with palladium acetate (168 mg, 0.75 mmol) in CH<sub>2</sub>Cl<sub>2</sub> (5 mL) at 24 °C for 48 h. The solvent was removed with a rotary evaporator to give a pale green complex 9a. This complex is highly soluble in *n*-pentane, even at −18 °C. The crude complex 9a was stirred in trifluoroacetic anhydride (1 mL) for 24 h at room temperature. The excess of anhydride was removed with a rotary evaporator and the residue was washed with cold *n*-pentane (0.2 mL × 2) and dried under high vacuum to afford a green complex 10a as a mixture of two isomers in a 91:9 ratio (225 mg, 84% yield). The

complex was characterized by NMR spectroscopy.  $^1\text{H}$  NMR (400 MHz,  $\text{CD}_2\text{Cl}_2$ )  $\delta$  0.92 (s, 9H  $\times$  0.91), 1.02 (s, 9H), 1.05 (s, 9H  $\times$  0.09), 1.32 (s, 3H  $\times$  0.09), 1.46 (s, 3H  $\times$  0.91), 2.34 (d,  $J$  = 8.0 Hz, 1H  $\times$  0.91), 2.52 (d,  $J$  = 8.0 Hz, 1H  $\times$  0.09), 3.00 (d,  $J$  = 8.0 Hz, 1H  $\times$  0.09), 3.37 (d,  $J$  = 8.0 Hz, 1H  $\times$  0.91), 3.46 (d,  $J$  = 8.0 Hz, 1H), 4.21 (t,  $J$  = 8.0 Hz, 1H  $\times$  0.91), 4.27 (t,  $J$  = 8.0 Hz, 1H  $\times$  0.09), 4.56 (d,  $J$  = 8.0 Hz, 1H);  $^{13}\text{C}$  NMR (100 MHz,  $\text{CD}_2\text{Cl}_2$ )  $\delta$  14.0, 21.5, 22.5, 23.8, 24.9, 25.6, 25.8, 25.9, 26.0, 26.1, 34.4, 34.5, 34.7, 35.3, 50.4, 51.1, 70.3, 70.8, 71.2, 71.3, 184.9, 185.5.

**4.2. Crystallization of syn-(S,S)-10a.** The complex 10a was dissolved in *n*-pentane at room temperature and filtered through a Cameo 3N syringe filter (0.45  $\mu$ , 3 mm) (Osmonics Inc.) in a glass sample vial. The complex was crystallized as green prisms in 24 h at  $-18^\circ\text{C}$ . The green prismatic crystals were characterized by X-ray crystallography.

**4.3. Computational Methodology.** Geometries were optimized with B3LYP and the SDD basis set for Pd and the 6-31G(d) basis set for other atoms. Single point energies were calculated at the M06/SDD-6-311++G(d,p) level. The reported free energies and enthalpies include zero-point energies and thermal corrections calculated at 298 K with B3LYP/SDD-6-31G(d). All calculations were performed with Gaussian 09.<sup>28</sup>

## ■ ASSOCIATED CONTENT

### 📄 Supporting Information

Experimental procedures, characterization of the complex syn-(S,S)-10a, complete ref 28, and computational details. This material is available free of charge via the Internet at <http://pubs.acs.org>.

## ■ AUTHOR INFORMATION

### Corresponding Author

yu200@scripps.edu; houk@chem.ucla.edu

### Notes

The authors declare no competing financial interest.

## ■ ACKNOWLEDGMENTS

We gratefully acknowledge TSRI and NSF Center for Stereoselective C–H Functionalization (CHE-0943980) and the National Science Foundation (CHE-1059084, KNH) for financial support of this research. Calculations were performed on the Hoffman2 cluster at UCLA and the Extreme Science and Engineering Discovery Environment (XSEDE), which is supported by the NSF.

## ■ REFERENCES

- (1) (a) Hartwig, J. F. *Nature* **2008**, *455*, 314. (b) Hartwig, J. F.; Cook, K. S.; Hapke, M.; Incarvito, C. D.; Fan, Y. B.; Webster, C. E.; Hall, M. B. *J. Am. Chem. Soc.* **2005**, *127*, 2538. (c) Du Bois, J. *Chemtracts* **2005**, *18*, 1. (d) Periana, R. A.; Bhalla, G.; Tenn, W. J.; Young, K. J. H.; Liu, X. Y.; Mironov, O.; Jones, C. J.; Ziatdinov, V. R. *J. Mol. Catal. A* **2004**, *220*, 7. (e) Crabtree, R. H. *J. Organomet. Chem.* **2004**, *689*, 4083. (f) Stahl, S. S.; Labinger, J. A.; Bercaw, J. E. *Angew. Chem., Int. Ed.* **1998**, *37*, 2180. (g) Sen, A. *Acc. Chem. Res.* **1998**, *31*, 550. (h) Shilov, A. E.; Shul'pin, G. B. *Chem. Rev.* **1997**, *97*, 2879. (i) Ryabov, A. D. *Chem. Rev.* **1990**, *90*, 403.
- (2) Davies, H. M. L.; Beckwith, R. E. *J. Chem. Rev.* **2003**, *103*, 2861.
- (3) (a) Yu, J. Q.; Giri, R.; Chen, X. *Org. Biomol. Chem.* **2006**, *4*, 4041. (b) Daugulis, O.; Zaitsev, V. G.; Shabashov, D.; Pham, Q. N.; Lazareva, A. *Synlett* **2006**, 3382. (c) Lyons, T. W.; Sanford, M. S. *Chem. Rev.* **2010**, *110*, 1147.
- (4) (a) Garcia-Cuadrado, D.; de Mendoza, P.; Braga, A. A. C.; Maseras, F.; Echavarren, A. M. *J. Am. Chem. Soc.* **2007**, *129*, 6880. (b) Garcia-Cuadrado, D.; Braga, A. A. C.; Maseras, F.; Echavarren, A. M. *J. Am. Chem. Soc.* **2006**, *128*, 1066.

(5) Davies, D. L.; Donald, S. M. A.; Macgregor, S. A. *J. Am. Chem. Soc.* **2005**, *127*, 13754.

(6) Gorelsky, S. I.; Lapointe, D.; Fagnou, K. *J. Am. Chem. Soc.* **2008**, *130*, 10848.

(7) (a) Lafrance, M.; Gorelsky, S. I.; Fagnou, K. *J. Am. Chem. Soc.* **2007**, *129*, 14570. (b) Lafrance, M.; Rowley, C. N.; Woo, T. K.; Fagnou, K. *J. Am. Chem. Soc.* **2006**, *128*, 8754. (c) Rousseaux, S.; Gorelsky, S. I.; Chung, B. K. W.; Fagnou, K. *J. Am. Chem. Soc.* **2010**, *132*, 10692. (d) Balcells, D.; Clot, E.; Eisenstein, O. *Chem. Rev.* **2010**, *110*, 749. (e) Ke, Z.; Cundari, T. R. *Organometallics* **2010**, *29*, 821. (f) Musaev, D. G.; Kaledin, A.; Shi, B. F.; Yu, J. Q. *J. Am. Chem. Soc.* **2012**, *134*, 1690.

(8) (a) Gomez, M.; Granell, J.; Martinez, M. *J. Chem. Soc., Dalton Trans.* **1998**, 37. (b) Ryabov, A. D.; Sakodinskaya, I. K.; Yatsimirsky, A. K. *J. Chem. Soc., Dalton Trans.* **1985**, 2629.

(9) (a) Giri, R.; Liang, J.; Lei, J. G.; Li, J. J.; Wang, D. H.; Chen, X.; Naggar, I. C.; Guo, C. Y.; Foxman, B. M.; Yu, J. Q. *Angew. Chem., Int. Ed.* **2005**, *44*, 7420. (b) Giri, R.; Chen, X.; Yu, J. Q. *Angew. Chem., Int. Ed.* **2005**, *44*, 2112. (c) Dick, A. R.; Kampf, J. W.; Sanford, M. S. *J. Am. Chem. Soc.* **2005**, *127*, 12790. (d) Powers, D. C.; Ritter, T. *Nat. Chem.* **2009**, *1*, 302. (e) Powers, D. C.; Geibel, M. A. L.; Klein, J. E. M. N.; Ritter, T. *J. Am. Chem. Soc.* **2009**, *131*, 17050. (f) Khusnutdinova, J. R.; Rath, N. P.; Mirica, L. M. *J. Am. Chem. Soc.* **2010**, *132*, 7303.

(10) Giri, R.; Shi, B.-F.; Engle, K. M.; Mangel, N.; Yu, J.-Q. *Chem. Soc. Rev.* **2009**, *38*, 3242.

(11) (a) Whitesides, T. H.; Arhart, R. W. *Tetrahedron Lett.* **1972**, *13*, 297. (b) Schroder, D.; Schwarz, H. *J. Am. Chem. Soc.* **1993**, *115*, 8818. (c) Schroder, D.; Zummack, W.; Schwarz, H. *J. Am. Chem. Soc.* **1994**, *116*, 5857. (d) Loos, J.; Schroder, D.; Zummack, W.; Schwarz, H. *Int. J. Mass Spectrom.* **2002**, *217*, 169. (e) Hornung, G.; Schroder, D.; Schwarz, H. *J. Am. Chem. Soc.* **1997**, *119*, 2273. (f) Ma, Y. O.; Bergman, R. G. *Organometallics* **1994**, *13*, 2548. (g) Mobley, T. A.; Bergman, R. G. *J. Am. Chem. Soc.* **1998**, *120*, 3253.

(12) Keyes, M. C.; Young, V. G.; Tolman, W. B. *Organometallics* **1996**, *15*, 4133.

(13) Johnson, J. A.; Ning, L.; Sames, D. *J. Am. Chem. Soc.* **2002**, *124*, 6900.

(14) (a) Eames, J.; Watkinson, M. *Angew. Chem., Int. Ed.* **2001**, *40*, 3567. (b) Covell, D. J.; White, M. C. *Angew. Chem., Int. Ed.* **2008**, *47*, 6448.

(15) (a) Groves, J. T.; Viski, P. *J. Am. Chem. Soc.* **1989**, *111*, 8537. (b) Larrow, J. F.; Jacobsen, E. N. *J. Am. Chem. Soc.* **1994**, *116*, 12129.

(16) (a) Thalji, R. K.; Ellman, J. A.; Bergman, R. G. *J. Am. Chem. Soc.* **2004**, *126*, 7192. (b) Harada, H.; Thalji, R. K.; Bergman, R. G.; Ellman, J. A. *J. Org. Chem.* **2008**, *73*, 6772.

(17) (a) Zalatan, D. N.; Du Bois, J. *J. Am. Chem. Soc.* **2008**, *130*, 9220. (b) Liang, J. L.; Yuan, S. X.; Huang, J. S.; Yu, W. Y.; Che, C. M. *Angew. Chem., Int. Ed.* **2002**, *41*, 3465.

(18) (a) Evans, D. A.; Bartroli, J.; Shih, T. L. *J. Am. Chem. Soc.* **1981**, *103*, 2127. (b) Meyers, A. I. *Acc. Chem. Res.* **1978**, *11*, 375. (c) Ellman, J. A.; Owens, T. D.; Tang, T. P. *Acc. Chem. Res.* **2002**, *35*, 984. (d) Myers, A. G.; Yang, B. H.; Chen, H.; McKinstry, L.; Kopecky, D. J.; Gleason, J. L. *J. Am. Chem. Soc.* **1997**, *119*, 6496.

(19) Meyers, A. I. *J. Org. Chem.* **2005**, *70*, 6137.

(20) Hargaden, G. C.; Guiry, P. J. *Chem. Rev.* **2009**, *109*, 2505.

(21) (a) Balavoine, G.; Clinet, J. C.; Zerbib, P.; Boubekour, K. *J. Organomet. Chem.* **1990**, *389*, 259. (b) Balavoine, G.; Clinet, J. C. *J. Organomet. Chem.* **1990**, *390*, C84.

(22) A part of the current research work has been published elsewhere : Giri, R., Ph.D. Thesis, The Scripps Research Institute, 2009.

(23) Moyano, A.; Rosol, M.; Moreno, R. M.; Lopez, C.; Maestro, M. A. *Angew. Chem., Int. Ed.* **2005**, *44*, 1865.

(24) Giri, R.; Chen, X.; Hao, X. S.; Li, J. J.; Liang, J.; Fan, Z. P.; Yu, J. Q. *Tetrahedron-Asymmetry* **2005**, *16*, 3502.

(25) Syn- and anti-geometries of the trinuclear palladacycles appear to be controlled by the steric bulk on both the oxazoline and the parent carboxylic acid moieties. However, the formation of syn- or



anti-geometry is irrelevant to the observed diastereoselectivity, since both geometries generate the same diastereomers.

(26) Gomez, M.; Granell, J.; Martinez, M. *Organometallics* **1997**, *16*, 2539.

(27) Palladium(II) acetate exists as a trimer in  $\text{CH}_2\text{Cl}_2$  and benzene solutions. For the determination of its solution phase structures, see:

(a) Stephens, T. A.; Morehous, S. M.; Powell, A. R.; Heffer, J. P.; Wilkinson, G. *J. Chem. Soc.* **1965**, 3632. (b) Bakhmutov, V. I.; Berry, J. F.; Cotton, F. A.; Ibragimov, S.; Murillo, C. A. *Dalton Trans.* **2005**, 1989.

(28) Frisch, M. J.; et al. *Gaussian 09, Rev. B.01*; Gaussian, Inc., Wallingford, CT, 2010.